doi:10.2533/chimia.2013.149 Chimia 67 (2013) 149–154

The Application of Electrospun Titania Nanofibers in Dye-sensitized Solar Cells

Hana Krysova[a], Arnost Zukal[a], Jana Trckova-Barakova[b], Aravind Kumar Chandiran[c], Mohammad Khaja Nazeeruddin[c], Michael Grätzel[c], and Ladislav Kavan*[a]

Abstract: Titania nanofibers were fabricated using the industrial Nanospider™ technology. The preparative protocol was optimized by screening various precursor materials to get pure anatase nanofibers. Composite films were prepared by mixing a commercial paste of nanocrystalline anatase particles with the electrospun nanofibers, which were shortened by milling. The composite films were sensitized by Ru-bipyridine dye (coded C106) and the solar conversion efficiency was tested in a dye-sensitized solar cell filled with iodide-based electrolyte solution (coded Z960). The solar conversion efficiency of a solar cell with the optimized composite electrode (η = 7.53% at AM 1.5 irradiation) outperforms that of a solar cell with pure nanoparticle film (η = 5.44%). Still larger improvement was found for lower light intensities. At 10% sun illumination, the best composite electrode showed η = 7.04%, referenced to that of pure nanoparticle film (η = 4.69%). There are non-monotonic relations between the film's surface area, dye sorption capacity and solar performance of nanofiber-containing composite films, but the beneficial effect of the nanofiber morphology for enhancement of the solar efficiency has been demonstrated.

Keywords: Dye-sensitized solar cells · Electrospinning · Titanium dioxide

1. Introduction

The dye-sensitized solar cell (DSC) presents an attractive alternative to solid-state photovoltaics at competitive cost.[1–4] The cells have a sandwich structure in which an electrolyte solution containing redox mediator is filled between a photoanode based on a thin film of dye-sensitized titanium dioxide and the counter electrode. Recent success in boosting the solar conversion efficiency was highlighted by replacement of the traditional I_3^-/I^- redox mediator by other couples with more positive electrochemical potentials[5–8] such as $Co^{3+/2+}$ complexes.[3,8–17] This strategy allowed demonstration of the champion (12.3 %) cell.[9] Counter electrodes are typically from platinized F-doped SnO_2 (FTO), but Pt can be replaced by cheaper materials, like carbons,[18] including electrospun carbon nanofibers.[19] Recently, graphene nanoplatelets[20–23] attracted considerable attention for this application.

Among various tasks to enhance the performance of DSC, the search for the best morphology of the semiconductor photoanode is one of the key research targets.[24,25] The strategy of using one-dimensional nanostructures is motivated by the assumption that the electron transport and collection are improved in 1D systems compared to the performance of the traditional nanostructures based on interconnected quasi-spherical particles.[26,27] Nair *et al.*[27] reviewed recently the use of 1D titania nanomaterials in DSC, concluding that they hold strong promise in enhancing the solar cell efficiency, but there is a lack of reliable and scalable synthetic methods for their commercial fabrication. Here we show that this problem can be addressed through the Nanospider™ technology,[28] which allows the production of electrospun titania in upscalable quantities at industrial level.

In general, electrospinning is a versatile method to produce polymeric fibers with diameters smaller than 100 nm and lengths up to kilometers in extreme cases.[29–31] The morphology and properties of nanofibers depend on the polymer type and process parameters, such as molecular weight of the precursor, solvent, applied electric field strength, solution viscosity, and deposition distance.[31–33] The technique is extendable to fabrication of inorganic materials. Li and Xia[34] pioneered the preparation of titania nanofibers by electrospinning from solution of poly(vinyl pyrrolidone) and titanium isopropoxide. Later on, they prepared uniaxially aligned titania nanofibers *via* electrospinning.[35] Although the name 'nanofibers' is not without some terminological objections[36] it became too popular to be avoided as a keyword for denoting these materials. Electrospun titania exhibits interesting structural and optical properties[37] which find applications in a variety of areas including photoelectrochemical hydrogen production,[38] photocatalysis[39] and dye-sensitized solar cells.[32,40–46]

All the above-mentioned titania nanofibers were produced in a classical set up, where a high voltage was applied between a collector and capillary tip which jets the solution of polymer and titania precursor from a syringe. A principal innovation applied in this work consists in avoiding the syringe/capillary system, *i.e.* the electrospinning is carried out directly from the surface of a liquid film.[28] We have optimized the synthesis of electrospun titania by this approach, and subsequently, developed a method for producing thin-film electrodes for DSC photoanode. Most of the cited previous works report on pure nanofiber films, which were deposited either directly on FTO[32,40,42,43] or pre-deposited TiO_2,[46] doctor bladed from a paste[45] or annealed by hot pressing.[41,44] Here, we used an alternative synthetic protocol, reminiscent of the so-called 'brick&mortar' strategy[47] which allowed us to improve the mechanical stability of nanofibrous electrodes. We succeeded in preparation of mechanically robust composite electrodes containing nanofibers and nanoparticles in various proportions. Thus formed TiO_2 nanofiber/nanoparticle composites were character-

*Correspondence: Dr. L. Kavan[a]
E-mail: kavan@jh-inst.cas.cz
[a]J. Heyrovský Institute of Physical Chemistry, v.v.i.
Academy of Sciences of the Czech Republic
Dolejškova 3, CZ-18223 Prague 8, Czech Republic
[b]ELMARCO, s.r.o.
V Horkach 76/18, CZ-460 07 Liberec, Czech Republic
[c]Laboratory of Photonics and Interfaces
Institute of Chemical Sciences and Engineering
Swiss Federal Institute of Technology,
CH-1015 Lausanne

ized by X-ray diffraction (XRD), scanning electron microscopy (SEM), adsorption isotherms of nitrogen or krypton, evaluated by Brunauer-Emmett-Teller method (BET), thermogravimetric analysis (TGA), and dye adsorption. The optimized composites were tested as photoanode materials in DSC.

2. Experimental Section

2.1 *Preparation of Nanofibers*

Nanofibers were prepared by electrospinning from appropriate polymer templates and Ti-precursors by the Nanospider™ technology.[28] Different polymer carriers were tested to control the products' properties (fiber diameter, surface area, crystallinity): polyvinylpyrrolidone (PVP), hydroxypropylcellulose (HPC) with molar weights MW 100 000 and 370 000, polyethylene oxide and polyvinyl alcohol. TiO_2 fiber samples (ET1-ET8) were electrospun from a mixture containing polymer, titanium alkoxide sol and stabilizers (acetylacetone) in ethanol or in ethanol/water mixture under controlled conditions (temperature and humidity) which are proprietary of Elmarco. The prepared electrospun TiO_2 fibers were calcined at temperatures from 350–590°C.

2.2 *Preparation of Nanoparticle/Nanofiber Composite Films for Electrodes*

The annealed nanofibers (see above) were milled, ultrasonically dispersed in ethanol and mixed with a paste of nanocrystalline anatase particles. The used paste was either the standard 18NR-T product (Dyesol) or custom-made lower viscosity pastes (ZA and ZB; Dyesol). The pastes were mixed with milled nanofibers with 0%, 5%, 10%, 20%, 50% and 75% or 80% of nanofibers (in wt%, calculated on TiO_2 basis). The final mixtures were subjected to ultrasonic treatment and stirring to prepare homogenous pastes. FTO glass slides (TEC 8 from Libbey-Owens-Ford, 8Ω/sq) were washed with ethanol and acetone. The films were deposited by the doctor blade technique on FTO, with Kapton foil tape defining the TiO_2 film borders and leaving a free FTO edge for electrical contact. The film was dried in air for 24 h and subsequently calcined at 450 °C for 60 min.

2.3 *Characterization Methods*

SEM images of nanofibers and composites were obtained by a Hitachi S-4800 microscope or Nova NanoSEM 230, FEI microscope. The BET surface areas of powder nanofibers samples were determined from nitrogen adsorption isotherms at 77 K using the Micromeritics ASAP 2020 Instrument and Nova 4000, Quantachrome. For the adsorption measurements on FTO-supported thin films, the isotherms of krypton at 77 K were measured using our previously developed method.[48,49] Before the adsorption measurement, all samples were degassed at 523 K overnight. The BET surface areas were calculated using the data in the range of relative pressure p/p_0 from 0.05 to 0.25. Following the usual practice, the saturation vapor pressure p_0 of the supercooled liquid krypton and the atomic cross-sectional area of 0.202 nm^2 were used. The film thickness was measured by DEKTAK profilometer. TGA analysis was performed by Netzsch STA449F1 thermogravimeter.

The Ru-bipyridine dye coded N719; chemical name: di-tetrabutylammonium *cis*-bis(isothiocyanato)bis(2,2'-bipyridyl-4,4' dicarboxylato) ruthenium(II) was used as a model molecule to investigate the adsorption properties of TiO_2 films. The procedure was as follows: warm (*ca.* 50 °C) TiO_2 electrodes were dipped in 4×10^{-4} M solution of N719 in acetonitrile + t-butanol (1/1, v/v) for 24 h. Then the electrodes were washed in acetonitrile + t-butanol to remove weakly bonded dye molecules. To determine the amount of chemically bonded dye N719, it was desorbed into phosphate buffer (pH 7.2) and the resulting solution was analyzed by UV-VIS spectrophotometry.[48] Measurements were performed in a 1 cm quartz cell on a spectrophotometer Lambda 19 (Perkin-Elmer).

For photoelectrochemical tests of experimental DSCs, the light source was a 450 W xenon light source (Osram XBO 450, Germany) with a filter (Schott 113). The light power was regulated to the AM 1.5 G solar standard by using a reference Si photodiode equipped with a color-matched filter (KG-3, Schott) to reduce the mismatch between the simulated light and AM 1.5 G to less than 4% in the wavelength region of 350–750 nm. The differing intensities were regulated with neutral wire mesh attenuator. The applied potential and cell current were measured using a Keithley model 2400 digital source meter.

2.4 *Assembly of Solar Cells*

The experimental DSC was assembled as follows: The TiO_2 thin film on FTO glass slides was scraped leaving an area of about 0.5×0.5 cm^2 and the films were calcined at 450 °C for 30 min. Immediately after the thermal treatment the still warm electrode (*ca.* 50 °C) was dipped into a solution of C106 dye; chemical name: NaRu(4,4-bis(5-(hexylthio)thiophen-2-yl)-2,2-bipyridine) (4-carboxylic acid-4-carboxylate-2,2-bipyridine) $(NCS)_2$. The C106 dye was chosen for the DSC tests due to its larger extinction coefficient and red-shifted spectral maximum compared to N719.[50] The C106 dye solution was 3×10^{-4} M in 10% DMF + 90% (1/1 acetonitrile/t-butanol mixture). After withdrawal, the film was washed with acetonitrile/t-butanol solution to remove weakly bonded dye, and dried in air at ambient temperature. The DSC was assembled with a counter electrode from platinized FTO, which was prepared by deposition of 5 μL/cm^2 of 10 mM H_2PtCl_6 in 2-propanol and calcination at 400 °C for 15 min. The cell was assembled using a Surlyn tape as a seal, and filled with an electrolyte solution, which was added through a hole in the counter electrode and finally closed with Surlyn seal. The electrolyte solution was Z960; it was composed of 1 M 1,3-dimethylimidazolium iodide, 50 mM LiI, 30 mM I_2, 0.5 M *tert*-butylpyridine, and 0.1 M guanidinium thiocyanate in a solvent mixture of 85% acetonitrile with 15% valeronitrile by volume. The cell active area for illumination was defined by a mask.

3. Results and Discussion

3.1 *Nanofibers*

In our initial attempts towards nanofibers synthesis, we adopted the protocol of Li and Xia[34] using polyvinylpyrrolidone (PVP) as the polymeric template. Solutions for fabrication of nanofibers were selected based on their viscosity, conductivity, and ability to be electrospun. The electrospun nanofibers were calcined at temperatures from 350–590 °C and characterized by SEM (fiber diameter), adsorption isotherms (BET surface area) and XRD analysis. The properties of the resulting TiO_2 nanofibers are summarized in Table 1. SEM images of the fibers templated with PVP are shown in Fig. 1. (Fibers templated with HPC look similar). Apparently, the surface areas of nanofibers do not scale with the fiber diameters, which matches the conclusion of other authors.[46] Nanofibers ET3 have similar diameters as ET1 but two times higher surface area. On the other hand, nanofibers ET2 have similar surface area as nanofibers ET1 though the diameter is two times smaller. It suggests that the porosity of nanofibers increases in the order ET2, ET1, ET3 which can be explained by an effect of increasing calcination temperature. The BET surface areas of our PVP-templated fibers (ET1-ET3) are comparable to those reported by Jung *et al.*[46] using a similar synthetic protocol. Furthermore, these authors added glycerine to the precursor mixture, which enhanced the product's porosity and surface areas considerably.[46]

For preparation of TiO_2 electrodes on top of FTO supports, calcination is necessary to remove organic additives from pre-

Table 1. Properties of TiO_2 nanofibers prepared with polyvinylpyrrolidone (PVP) or hydroxypropylcellulose (HPC) as polymer carrier and calcined at various temperatures. Surface areas were determined from N_2-adsorption isotherms by BET method.

Nanofiber	Polymer template	Calcination temperature [°C]	Fiber diameter [nm]	Surface area [m^2/g]
ET1	PVP	550	300	16
ET2	PVP	530	150	15
ET3	PVP	590	280	35
ET4	HPC	450	240	30
ET5	HPC	450	310	90
ET6	HPC	450	250	60
ET7	HPC	350	250	145
ET8	HPC	450	380	80

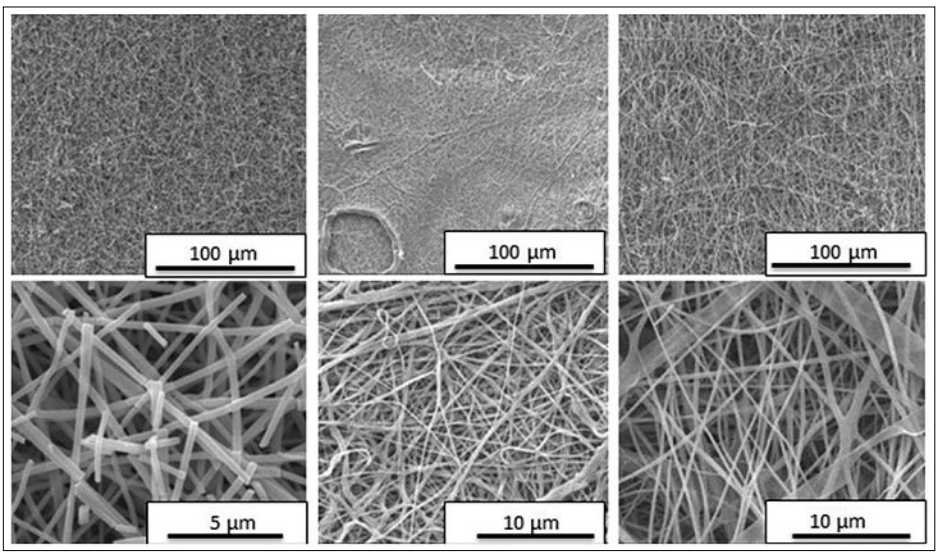

Fig. 1. SEM images of titanium dioxide fiber samples templated with PVP. (Left column: ET1, middle column: ET2, right column: ET3).

vious synthetic steps, but the temperature of *ca.* 450–500 °C should not be exceeded.[24] Thermogravimetric analysis (TGA) was performed to check for completeness of removal of polymeric templates. Fig. 2 shows that calcination of PVP is incomplete at these temperatures (*cf.* also ref. [46]): about 30% of the non-pyrolyzed residue remains at 450 to *ca.* 650 °C. To find other polymer carriers with lower burning temperatures, we screened hydroxypropylcellulose (HPC), polyethylene oxide and polyvinyl alcohol. The best results were obtained for HPC; its thermogravimetric analysis (Fig. 2) showed that at 540 °C the residue was only 1.4% and at 450 °C it was only about 3%. As a result of these tests, HPC was chosen for preparation and optimization of titanium dioxide nanofibers for DSC application. Powder X-ray diffraction indicated pure anatase in the samples calcined at 450–590 °C (an example is shown in Fig. 3) but samples calcined at 350 °C turned out to be amorphous. Effect of the calcination temperature on the surface area of nanofibers was investigated for nanofibers ET7 (Fig. 4). Obviously, the effect of re-calcination at higher temperature is significant (Fig. 4).

3.2 *Composite Nanoparticle/ Nanofiber*

Calcined nanofibers were typically a few millimeters long, but the thickness of the TiO_2 layers used for DSC applications is usually between *ca.* 5 and 20 µm.[24] Consequently, the efficient connection of particles and fibers in the film requires shortening of the length of fibers. To decrease the length of TiO_2 nanofibers, they were milled for varying times (10, 30, 60 and 120 s) in liquid nitrogen. The morphology of milled nanofibers is shown in Fig. 5. Milling of nanofibers longer than 120 s breaks them into small particles with lengths comparable with the diameter. After milling for 30 s the length is similar to the thickness of the final electrode layer. Hence, this was chosen as the optimum milling time.

The composites were prepared by mixing commercial paste (nanocrystalline anatase particles from Dyesol) with 0%, 5%, 10%, 20%, 50% and 75% or 80% milled nanofibers. The composite electrodes from standard Dyesol paste (DSL 18 NR-T) were of poor quality, particularly for composites with a larger proportion of nanofibers, which did not stick well to the FTO supports. However, custom-made lower viscosity pastes ZA and ZB (Dyesol) behaved better; they provided homogeneous composites with satisfactory mechanical properties and good adhesion to the support. The nanofibers which were milled at

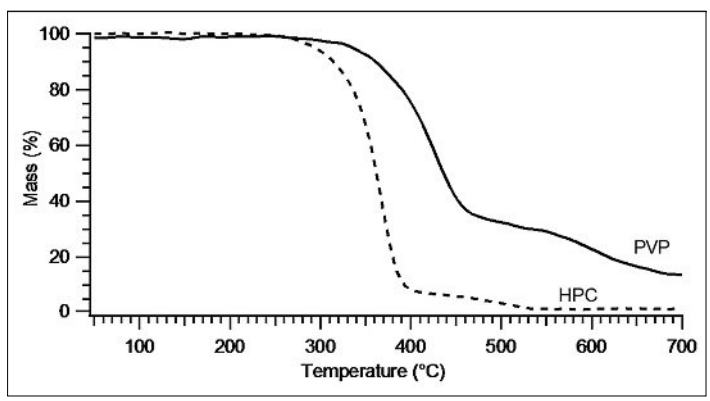

Fig. 2. Thermogravimetric analysis of polyvinylpyrrolidone (PVP) and hydroxypropylcellulose (HPC).

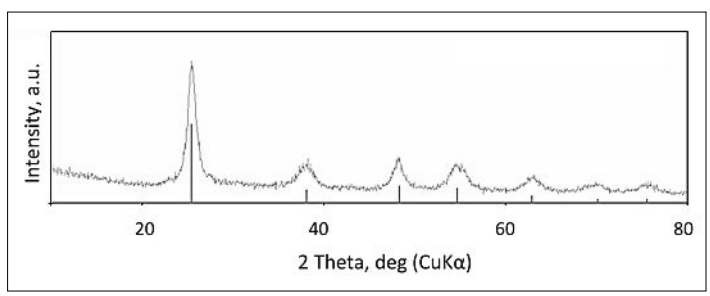

Fig. 3. XRD pattern of titanium dioxide fiber (sample ET6).

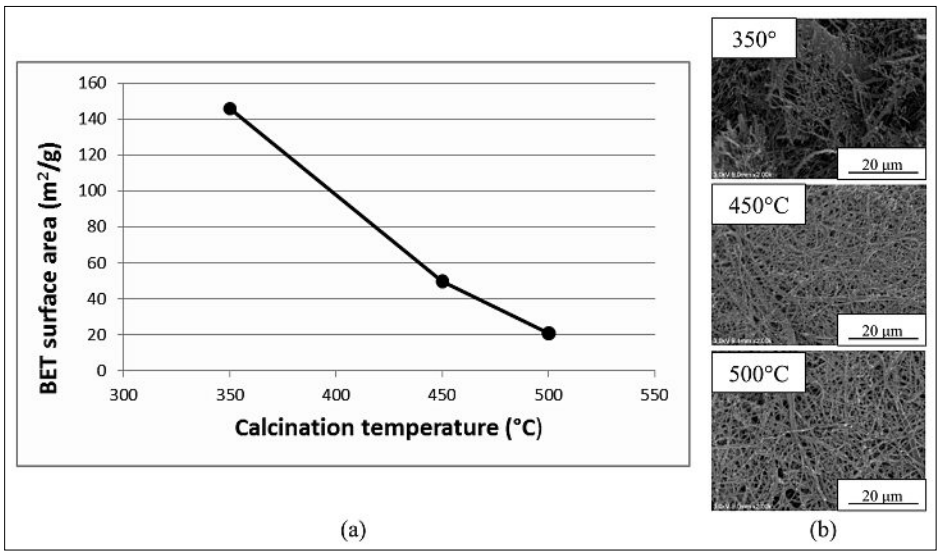

Fig. 4. (a) Dependence of BET specific surface area of ET7 nanofibers on calcination temperature (heating rate 10°C/min), (b) SEM images of TiO_2 nanofibers after re-calcination at 350, 450 and 500 °C.

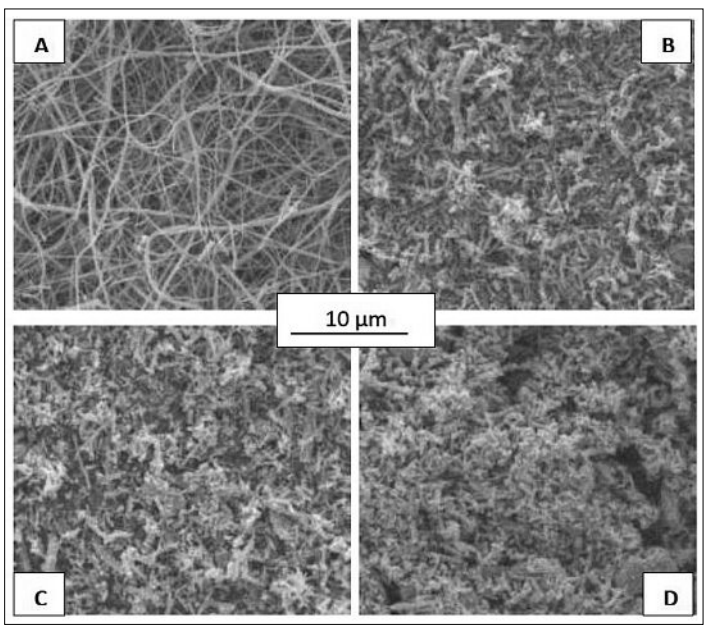

Fig. 5. SEM images of milled electrospun TiO_2 nanofibers (ET3). Milling time (A) 0 s, (B) 30 s, (C) 60 s, (D) 120 s.

optimized conditions (*cf.* Fig. 5B) are statistically oriented in the composite. Hence, there is a certain amount of fibers vertical to the surface, and they enhance the charge transport most efficiently.

Addition of TiO_2 fibers influenced the electrode layer thickness and mass (Fig. 6). The larger the proportion of nanofibers, the higher the layer thickness. Layer thicknesses for the same proportion of nanofibers were different for individual nanofibers. For instance, the layer thickness of a 20% ET6 composite was 7.5 µm and that of 20% ET5 composite was 9 µm (Table 2). Nevertheless, the mass of the deposited composite per cm^2 was similar (the layer mass of 20% ET6 was 0.975 mg/cm^2 and that of ET5 was 0.984 mg/cm^2). SEM images in Fig. 7 demonstrate that the composites are reasonably uniform, with the nanofibers homogeneously interspersed with the anatase nanoparticles acting as binder.

To determine the adsorption capacity of our thin film electrodes, we used two compatible techniques: Kr-adsorption isotherms, which provided accurate data directly for FTO-supported thin-film electrodes[48,49] and spectrophotometrical quantification of the adsorbed amount of model dye N719. The reason for choosing N719 for investigation of adsorption properties consists in detailed knowledge of the surface anchoring of this dye to titania surfaces[51] and the possibility of comparison with earlier works[48] including those on electrospun titania.[40,41] Some other works reported on electrospun titania in combination with a similar dye, N3.[32,42] The representative data for various composites are summarized in Table 2 and Fig. 8.

The adsorption capacity for N719 decreased almost proportionally with increasing percentage of nanofibers in the film, independent of the fiber type. Surprisingly, this trend is not reproduced for the Kr-adsorption (expressed in the units of roughness factor, Rf) but it is just the opposite. Even if we consider small fluctuations in the film thickness (Table 2) the increase of Rf for fiber-containing composites is significant. This leads to an assumption that the fibrous composites have fractal character. Whereas krypton atoms can be adsorbed on small irregularities of the surface, large molecules like N719 are too big to detect small surface roughness. Therefore, the amount of adsorbate necessary to form a monolayer depends on the size of the molecule and on the fractal dimension of the surface.[52] The discussion of molecular size vs. the adsorption capacity is further illustrated by experimental value of surface coverage of titania by N719 which was found to be be-

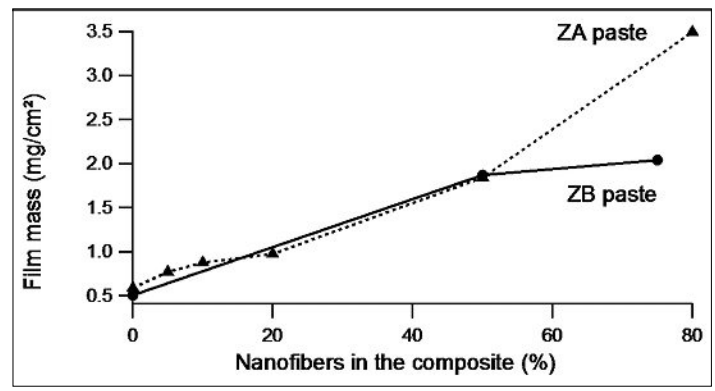

Fig. 6. Effect of the nanofiber concentration in the paste on layer mass: comparison of the specific mass of the layer for different amount of added nanofibers (ET6) for two different types of pastes: paste ZA and paste ZB.

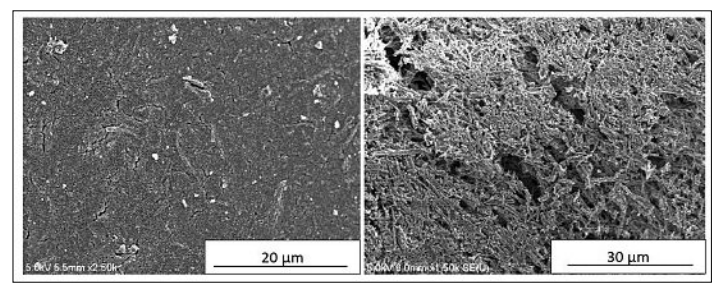

Fig. 7. SEM images of composites with 20% of nanofibers ET6 in paste ZA (right), and 80% (left) of NF in ZB paste.

Table 2. Properties of selected composite electrodes for DSC applications. The roughness factor, Rf was calculated as a ratio of the physical surface area of the TiO_2 composite electrode (determined from krypton adsorption isotherm) and the projected electrode area. The adsorption capacity for N719 dye was normalized to the TiO_2 mass per projected electrode area. For comparison, reference data are shown for a fiber-free film made from pure paste ZA.

	Fiber diameter [nm]	Film thickness [μm]	Rf	Dye N719 adsorption [μmol/cm²g]
paste ZA	-	6.5	558	111.6
5% ET6 in ZA	250	7	650	91.6
10% ET6 in ZA	250	7.3	715	81.1
20% ET6 in ZA	250	7.5	710	73.5
20% ET5 in ZA	310	9	985	69.7

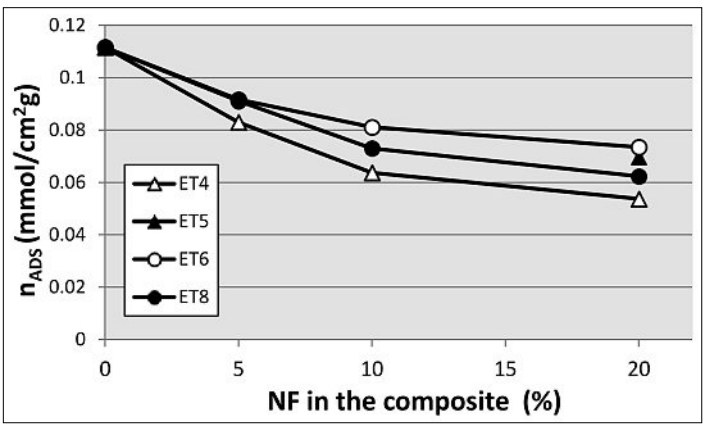

Fig. 8. Dye N719 adsorption as a function of nanofiber concentration in composite films prepared with paste ZA.

tween 0.73 and 1.3 molecules/nm²[53] and similar values were reported for N3, between 0.56 and 1.16 molecules/nm².[54–59] The situation is quite reminiscent of the Pluronic-templated films, where about one third of the ideal coverage for a perfect monolayer of N719 was found.[48] On the other hand, Lee *et al.*[40] reported better sorption of N719 on their electrospun titania nanorods (85.9 μmol/g-TiO_2) compared to that on nanoparticles (34.4 μmol/g-TiO_2). We do not comment on this discrepancy here, but note that the extinction coefficient of N719 used in the cited work[40] (ε_{535} = 3478 $cm^{-1}M^{-1}$) does not seem to be correct.[48,49]

Even though the dye sorption is not ideal on the total surface of composites (see above) the improvement in solar conversion efficiency in experimental DSCs was found to be significant. Table 3 summarizes the representative data for optimized composite electrodes and for comparison, fiber-free electrode (ZA) was also tested at the same conditions. Closer inspection of the data in Tables 2 and 3 demonstrates that there are no simple monotonic trends between the dye (or Kr) sorption capacity and solar performance. The highest solar efficiency of the composites was obtained for 20% ET6 composite (η = 7.53%), for 20% ET5 composite was lower (η = 6.03%). The dye adsorption capacity was slightly larger for the best composite film: 73.5 μmol/cm²g vs. 69.7 μmol/cm²g for the electrodes 20% ET6, compared to 20% ET5, respectively. However, the dye adsorption capacity of this optimum electrode was smaller than that of the reference fiber-free electrode (111.6 μmol/cm²g) which exhibited quite low solar performance (η = 5.44%). This illustrates the fact that the special fibrous morphology is, indeed, beneficial for the DSC performance. This finding matches those of some previous works[32,40,41] reporting on improved performance of electrospun nanofibers in various systems. Larger improvement is detected for smaller light intensities: *e.g.* at 10% sun, our best composite electrode showed η = 7.04%, referenced to that of pure nanoparticle film (η = 4.69%). Our efficiencies compare favorably to those found earlier[46] for electrodes with PVP-templated electrospun TiO_2 fibers sensitized with N719 dye (note a possible typo in the dye code, which is given in the cited paper[46]).

Table 3. Solar efficiency of DSC with a photoanode fabricated from pure paste ZA and with photoanodes from optimized composites containing nanofibers.

	Solar conversion efficiency, η		
	10% Sun	50% Sun	100% Sun
Paste ZA	4.11%	5.34%	5.44%
20% ET6 in paste ZA	7.04%	7.17%	7.53%
20% ET5 in paste ZA	4.69%	5.83%	6.03%

4. Conclusion

The preparation of titania nanofibers was optimized by screening various precursor materials. Calcination at 450 °C forms anatase crystals of TiO_2 but the temperature is not high enough to remove PVP polymer. Thermogravimetric analysis showed residue of 30% of PVP after calcination at 500 °C. The best properties were exhibited by hydroxypropylcellulose as a polymer carrier, for which the detemplating by air calcination at 450 °C was almost perfect. The range of fiber diameters was 150 to 380 nm and surface areas from 15 to 145 m^2/g.

Composite films were prepared by mixing the electrospun nanofibers, which were shortened by milling under liquid nitrogen. The best materials were obtained by using the custom-made low viscosity pastes (ZA and ZB) from Dyesol.

The composite films were sensitized by C106 dye and the solar conversion efficiency was tested in model DSCs with Z960 electrolyte. The actual value of efficiency of the optimized composite electrode (7.53% at AM 1.5 irradiation) outperforms that of pure nanoparticle film (5.44%) in spite of various non-monotonic trends between Kr-, dye-adsorption capacity and solar efficiency. Larger improvement is detected for lower light intensities: *e.g.* at 10% sun, the best composite electrode shows 7.04% efficiency, referenced to that of pure nanoparticle film (4.11%).

Acknowledgements

This work was funded by the European Community's Programme FP7 under grant agreement No. 246124, SANS project and NMP-229036 ORION project. LK acknowledges the financial contribution from Academy of Sciences of the Czech Republic (contracts IAA 400400804 and KAN 200100801). The work of AZ was supported by the Grant Agency of the Czech Republic (GACR 203/08/0604). Thanks are due to Dr. Zhihong Cai (Dyesol) for custom-made pastes ZA and ZB.

Received: December 21, 2012

[1] M. Grätzel, *Nature* **2001**, *414*, 338.
[2] K. Kalyanasundaram, 'Dye Sensitized Solar Cells', CRC Press Taylor & Francis, Boca Raton, **2010**.
[3] B. E. Hardin, H. J. Snaith, M. D. McGehee, *Nature Photonics* **2012**, *6*, 161.
[4] A. Hagfeldt, G. Boschloo, L. Sun, L. Kloo, H. Pettersson, *Chem. Rev.* **2010**, *110*, 6595.

[5] M. Wang, N. Chamberland, L. Breau, J. Moser, R. Humphry-Baker, B. Marsan, S. M. Zakeeruddin, M. Grätzel, *Nature Chem.* **2010**, *2*, 385.
[6] T. Daeneke, T. H. Kwon, A. B. Holmes, N. W. Duffy, U. Bach, L. Spiccia, *Nature Chem.* **2011**, *3*, 211.
[7] T. W. Hamann, J. W. Ondersma, *Energy Environ. Sci.* **2011**, *4*, 370.
[8] J. Cong, X. Yang, L. Kloo, L. Sun, *Energy Environ. Sci.* **2012**, DOI: 10.1039/c2ee22095d.
[9] A. Yella, H. W. Lee, H. N. Tsao, C. Yi, A. K. Chandiran, M. K. Nazeeruddin, E. W. G. Diau, C. Y. Yeh, S. M. Zakeeruddin, M. Grätzel, *Science* **2011**, *334*, 629.
[10] T. W. Hamann, *Dalton Trans.* **2012**, *41*, 3111.
[11] H. N. Tsao, J. Burschka, C. Yi, F. Kessler, M. K. Nazeeruddin, M. Grätzel, *Energy Environ. Sci.* **2011**, *4*, 4921.
[12] S. Ahmad, T. Bessho, F. Kessler, E. Baranoff, J. Frey, C. Yi, M. Grätzel, M. K. Nazeeruddin, *Phys. Chem. Chem. Phys.* **2012**, *14*, 10631.
[13] S. M. Feldt, E. A. Gibson, E. Gabrielsson, L. Sun, G. Boschloo, A. Hagfeldt, *J. Am. Chem. Soc.* **2010**, *132*, 16714.
[14] H. N. Tsao, C. Yi, T. Moehl, J.-H. Yum, S. M. Zakeeruddin, M. K. Nazeeruddin, M. Grätzel, *Chem. Sus. Chem.* **2011**, *4,* 591.
[15] D. Zhou, Q. Yu, N. Cai, Y. Bai, Y. Wang, P. Wang, *Energy Environ. Sci.* **2011**, *4*, 2030.
[16] J. Liu, J. Zhang, M. Xu, D. Zhou, X. Jing, P. Wang, *Energy Environ. Sci.* **2011**, *4*, 3021.
[17] J.-H. Yum, E. Baranoff, F. Kessler, T. Moehl, S. Ahmad, T. Bessho, A. Marchioro, E. Ghadiri, J. E. Moser, M. K. Nazeeruddin, M. Grätzel, *Nature Comm*. **2012**, *3*, 631.
[18] T. N. Murakami, M. Grätzel, *Inorg. Chim. Acta* **2008**, *361*, 572.
[19] P. Joshi, L. Zhang, Q. Chen, D. Galipeau, H. Fong, Q. Qiao, *ACS Appl. Mat. Interfac.* **2010**, *2*, 3572.
[20] J. D. Roy-Mayhew, D. J. Bozym, C. Punckt, A. Aksay, *ACS Nano* **2010**, *10*, 6203.
[21] L. Kavan, J.-H. Yum, M. Grätzel, *ACS Nano* **2011**, *5*, 165.
[22] L. Kavan, J.-H. Yum, M. Grätzel, *Nano Lett.* **2011**, *11*, 5501.
[23] L. Kavan, J.-H. Yum, M. K. Nazeeruddin, M. Grätzel, *ACS Nano* **2011**, *5*, 9171.
[24] L. Kavan, in 'Dye-sensitized Solar Cells', Ed. K. Kalyanasundaram, CRC Press Taylor & Francis, Boca Raton, **2010**, pp. 45-81.
[25] L. Kavan, *Chem. Rec.* **2012**, *12*, 131.
[26] M. Law, L. E. Greene, J. C. Johnson, R. Saykaly, P. Yang, *Nature Mat.* **2005**, *4*, 455.
[27] A. S. Nair, Z. Peining, J. Babu, Y. Shengyuan, S. Ramakrishna, *Phys. Chem. Chem. Phys.* **2011**, *13*, 21248.
[28] O. Jirsak, O. Sanetrnik, D. Lukas, V. Kotek, L. Martinova, J. Chaloupek, 'A Method of Nanofibres Production from a Polymer Solution Using Electrostatic Spinning and Device for Carrying out the Method', US Pat. 7,585,437, **2005**.
[29] A. Frenot, I. S. Chronakis, *Curr. Op. Colloid Interfac. Sci.* **2003**, *8*, 64.
[30] M. Bognitzki, W. Czado, T. Frese, A. Schaper, M. Hellwig, M. Steinhart, A. Greiner, J. H. Wendorff, *Adv. Mater.* **2001**, *13*, 70.
[31] A. Greiner, J. H. Wendorff, *Angew. Chem. Int. Ed.* **2007**, *46*, 5670.
[32] M. Y. Song, D. K. Kim, S. M. Jo, D. Y. Kim, *Synth. Metals* **2005**, *155*, 635.
[33] J. M. Deitzel, J. Kleinmeyer, D. Harris, N. C. Beck Tan, *Polymer* **2001**, *42*, 261.
[34] D. Li, Y. Xia, *Nano Lett.* **2003**, *3*, 555.
[35] L. Wan, S. Wang, X. Wang, B. Dong, Z. Xu, X. Zhang, Y. Bing, S. Peng, J. Wang, C. Xu, *Solid State Sci.* **2011**, *13*, 468.
[36] M. Zukalova, J. Prochazka, Z. Bastl, J. Duchoslav, L. Rubacek, D. Havlicek, L. Kavan, *Chem. Mater*. **2010**, *22*, 4045.
[37] A. Kumar, R. Jose, K. Fujihara, J. Wang, S. Ramakrishna, *Chem. Mater.* **200**7, *19*, 6536.
[38] Y. L. Chen, Y. H. Chang, I. Chen, C. Kuo, *J. Phys. Chem. C* **2012**, *116*, 3857.
[39] S. Zhan, D. Chen, X. Jiao, C. Tao, *J. Phys. Chem. B* **2006**, *110*, 11199.
[40] B. H. Lee, M. Y. Song, S. M. Jo, S. Y. Kwak, D. Y. Kim, *J. Phys. Chem. C* **2009**, *113*, 21453.
[41] D. Hwang, S. M. Jo, D. Y. Kim, V. Armel, D. R. MacFarlane, S. Y. Jang, *ACS Appl. Mat. Interfac.* **2011**, *3*, 1521.
[42] M. Y. Song, D. K. Kim, K. J. Ihn, S. M. Jo, D. Y. Kim, *Synth. Metals* **2005**, *153*, 77.
[43] K. Onozuka, B. Ding, Y. Tsuge, T. Naka, M. Yamazaki, S. Sugi, M. Yoshikawa, S. Shiratori, *Nanotechnology* **2006**, *17*, 1026.
[44] H. Kokubo, B. Ding, T. Naka, H. Tsuchihira, S. Shiratori, *Nanotechnology* **2007**, *18*, 165604.
[45] P. S. Archana, R. Jose, T. M. Jin, C. Vijila, M. M. Yusoff, S. Ramakrishna, *J. Amer. Ceram. Soc.* **2010**, *93*, 4096.
[46] W. H. Jung, N. S. Kwak, T. S. Hwang, K. B. Yi, *Appl. Surf. Sci.* **2012**, *261*, 343.
[47] J. M. Szeifert, D. Fattakhova-Rohlfing, D. Georgiadou, V. Kalousek, J. Rathousky, D. Kuang, S. Wenger, S. M. Zakeeruddin, M. Grätzel, T. Bein, *Chem. Mater.* **2009**, *21*, 1260.
[48] M. Zukalova, J. Prochazka, A. Zukal, J.-H. Yum, L. Kavan, *Inorg. Chim. Acta* **2008**, *361*, 656.
[49] M. Zukalova, A. Zukal, L. Kavan, M. K. Nazeeruddin, P. Liska, M. Grätzel, *Nano Lett*. **2005**, *5*, 1789.
[50] Y. Cao, Y. Bai, Q. Yu, Y. Cheng, S. Liu, D. Shi, F. Gao, P. Wang, *J. Phys. Chem. C* **2009**, *113*, 6290.
[51] S. Fantacci, F. De Angelis, *Coord. Chem. Rev.* **2011**, *255*, 2704.
[52] P. Pfeiffer, D. Avnir, *J. Chem. Phys.* **1983**, *79*, 3558.
[53] L. Ellis-Gibbings, V. Johansson, R. B. Walsh, L. Kloo, J. S. Quinton, G. G. Andersson, *Langmuir* **2012**, *28*, 9431.
[54] L. Kavan, M. Grätzel, S. E. Gilbert, C. Klemenz, H. J. Scheel, *J. Am. Chem. Soc.* **1996**, *118*, 6716.
[55] V. Shklover, M. K. Nazeeruddin, S. M. Zakeeruddin, C. Barbe, A. Kay, T. Haibach, W. Steurer, R. Herman, H. U. Nissen, M. Grätzel, *Chem. Mater.* **1997**, *9*, 430.
[56] P. Persson, M. J. Lundqvist, *J. Phys. Chem. B* **2005**, *109*, 11918.
[57] A. Fillinger, B. A. Parkinson, *J. Electrochem. Soc.* **1999**, *146*, 4559.
[58] Y. Lu, D. Choi, J. Nelson, O. B. Yang, B. A. Parkinson, *J. Electrochem. Soc*. **2006**, *153*, E131.
[59] M. K. Nazeeruddin, S. M. Zakeeruddin, R. Humphry-Baker, M. Jirousek, P. Liska, N. Vlachopolous, V. Shklover, C. H. Fischer, M. Grätzel, *Inorg. Chem.* **1999**, *38*, 6298.